

SCIENTIFIC REPORTS



OPEN

Auditory metabolomics, an approach to identify acute molecular effects of noise trauma

Lingchao Ji¹, Ho-Joon Lee², Guoqiang Wan¹, Guo-Peng Wang¹, Li Zhang², Peter Sajjakulnukit², Jochen Schacht¹, Costas A. Lyssiotis¹ ² & Gabriel Corfas¹

Animal-based studies have provided important insights into the structural and functional consequences of noise exposure on the cochlea. Yet, less is known about the molecular mechanisms by which noise induces cochlear damage, particularly at relatively low exposure levels. While there is ample evidence that noise exposure leads to changes in inner ear metabolism, the specific effects of noise exposure on the cochlear metabolome are poorly understood. In this study we applied liquid chromatography-coupled tandem mass spectrometry (LC-MS/MS)-based metabolomics to analyze the effects of noise on the mouse inner ear. Mice were exposed to noise that induces temporary threshold shifts, synaptopathy and permanent hidden hearing loss. Inner ears were harvested immediately after exposure and analyzed by targeted metabolomics for the relative abundance of 220 metabolites across the major metabolic pathways in central carbon metabolism. We identified 40 metabolites differentially affected by noise. Our approach detected novel noise-modulated metabolites and pathways, as well as some already linked to noise exposure or cochlear function such as neurotransmission and oxidative stress. Furthermore, it showed that metabolic effects of noise on the inner ear depend on the intensity and duration of exposure. Collectively, our results illustrate that metabolomics provides a powerful approach for the characterization of inner ear metabolites affected by auditory trauma. This type of information could lead to the identification of drug targets and novel therapies for noise-induced hearing loss.

Noise-induced hearing loss (NIHL) affects more than 300 million people worldwide, and 10% of the world's population is exposed to potentially damaging sounds on a daily basis¹, making noise exposure one of the most common causes of sensorineural hearing loss. Noise can affect the inner ear in two main ways, either by directly damaging tissues through the physical forces brought on by the sound waves, or by inducing molecular changes that then impact the health and function of inner ear cells or neurons. The severity of acoustic trauma and the resulting NIHL depends on the intensity and the duration of noise exposure. Loud sounds might cause a permanent threshold shift, i.e. overt hearing loss (OHL), which has traditionally been well investigated in patients and animals. In this case, a broad set of structures in the cochlea can be damaged, including stereocilia, hair cells, supporting cells and even the tectorial membrane². Another type of NIHL that has received attention lately, hidden hearing loss (HHL)³, can occur upon exposure to moderate noise that only causes temporary shifts in hearing thresholds but permanently impairs sound-evoked neurotransmission, i.e. HHL is characterized by a decreased amplitude of the first peak of the auditory brain stem response (ABR) waveform that reflects the activation of the auditory nerve⁴. Noise-induced HHL is believed to be caused by the loss of synapses (synaptopathy) between inner hair cells and fibers of high-threshold spiral ganglion neuron⁵. Consequently, it has been suggested that HHL in humans leads to speech perception difficulties in noisy environments, while hearing thresholds remain normal^{6,7}.

Despite the enormous impact of NIHL, the molecular mechanisms by which noise trauma damages the inner ear remain inadequately understood. The effects of noise are usually very rapid, e.g. synaptopathy is evident immediately after a two-hour exposure⁸, suggesting that they are mediated by changes in metabolism, which can

¹Kresge Hearing Research Institute and Department of Otolaryngology - Head and Neck Surgery, University of Michigan Medical School, 48109, Ann Arbor, USA. ²Department of Molecular and Integrative Physiology, University of Michigan Medical School, 48109, Ann Arbor, USA. Lingchao Ji and Ho-Joon Lee contributed equally. Correspondence and requests for materials should be addressed to C.A.L. (email: clyssiot@med.umich.edu) or G.C. (email: corfas@med.umich.edu)

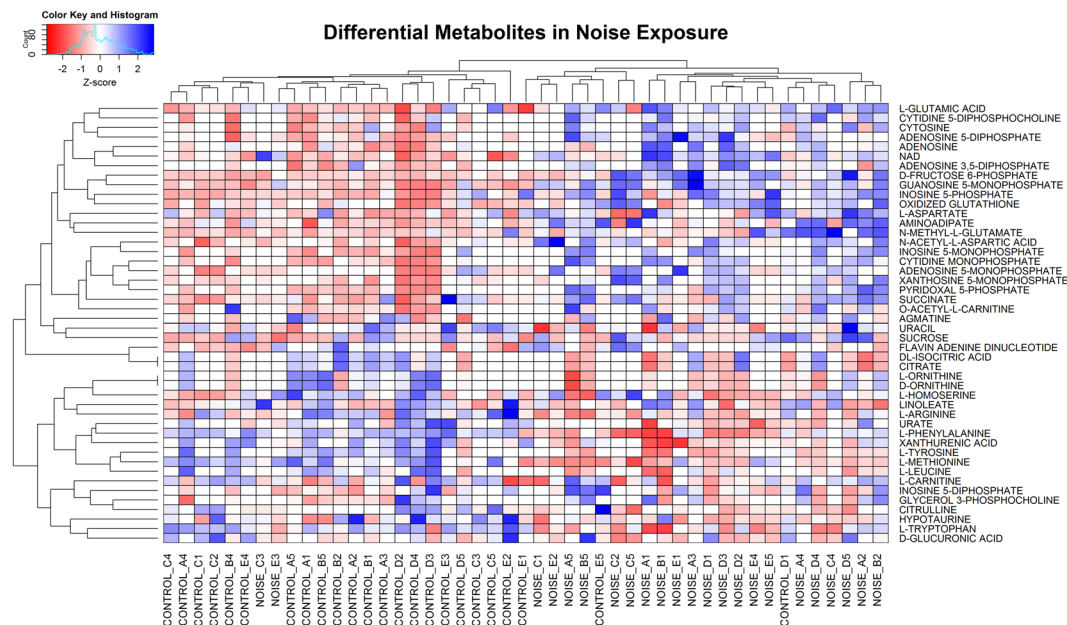


Figure 1. Differential metabolites and unsupervised hierarchical clustering. Data sets resulting from the LC-MS/MS runs of inner ears of control and noise-exposed mice (after filtering out under-loaded samples) were subjected to unsupervised hierarchical clustering. The control and noise-exposed samples segregate according to exposure with the exception of a few samples. The suffixes of “A1” to “E5” in the sample names represent 3 biological replicate experiments with each LC method and mice numbers: A = experiment 1 with RPLC, B = experiment 2 with RPLC, C = experiment 2 with HILIC, D = experiment 3 with RPLC, and E = experiment 3 with HILIC.

occur similarly rapidly, as opposed to resulting from effects on gene expression, which can take hours to manifest. Yet, little is known about the effects of noise on the inner ear metabolome. Previous work on metabolic changes associated with NIHL has focused on OHL and on candidate molecules known to be involved in central nervous system trauma, e.g. glutamate, reactive oxygen species (ROS) and inflammatory mediators^{9–14}. Unfortunately, pharmacological approaches targeting these pathways have not produced clinical treatments that effectively prevent noise-induced synaptopathy or hair cell loss, likely a reflection of the complexity of the biochemical changes induced. To better understand the effects of noise on the inner ear, we developed an auditory metabolomics pipeline that provides a comprehensive overview of the cochlear metabolome during noise exposure. Our results identified several metabolites and pathways influenced by noise, including some already linked to exposure or cochlear function, e.g. glutamate and NAD⁺, as well as numerous metabolites that have not been reported previously. This approach also shows that the effects of noise on the inner ear metabolome depend on the intensity and duration of the exposure. We believe that metabolomics is a powerful tool to define the ways in which the inner ear is affected by noise and will help identify the key molecular pathways that contribute to the different types of NIHL. This information would be helpful in guiding the design of new therapeutic approaches.

Results

Effects of an HHL-inducing noise exposure on the inner ear metabolome. To begin exploring the effects of noise on the mouse inner ear metabolome, we exposed CBA/J mice to a noise band of 8–16 kHz at 100 decibels sound pressure level (dB SPL) for 2 hours, which induces temporary threshold shifts, synaptopathy and permanent hidden hearing loss^{4,8}. We performed three biological replicate experiments, each with 5 animals per group (exposed and control). Temporal bones were harvested immediately after the exposure and the samples analyzed by liquid chromatography tandem mass spectrometry (LC-MS/MS). We measured the abundance of more than 220 metabolites which represent metabolic pathways in central carbon metabolism, including glycolysis, mitochondrial metabolism, amino acids, nucleotides, among others (see Methods section). We performed a two-tailed t-test to identify metabolites with significant differences between exposed and control samples in each experiment. Differential metabolites were defined as those with p-values < 0.1 and CV < 100% among replicates. This group of metabolites was considered for further analysis if they were consistent across the three experiments and present in at least 50% of all samples. These criteria identified 40 differential metabolites influenced by noise exposure. We then subjected this group of 40 metabolites to unsupervised hierarchical clustering (Fig. 1), which showed a good separation of control and noise-exposed samples. As shown in Fig. 2, this analysis identified 25 up-regulated and 15 down-regulated metabolites. The up-regulated metabolites include nucleotides, cofactors, and carbohydrates, as well as glutamate. Most of the down-regulated metabolites are amino acids such as methionine and arginine. Pathway analysis of the differential metabolites showed that up-regulation impacts most significantly alanine, aspartate, purine, glutamine and glutamate metabolism, while the down-regulated metabolites are involved in phenylalanine, tyrosine, and tryptophan metabolism (Table 1).

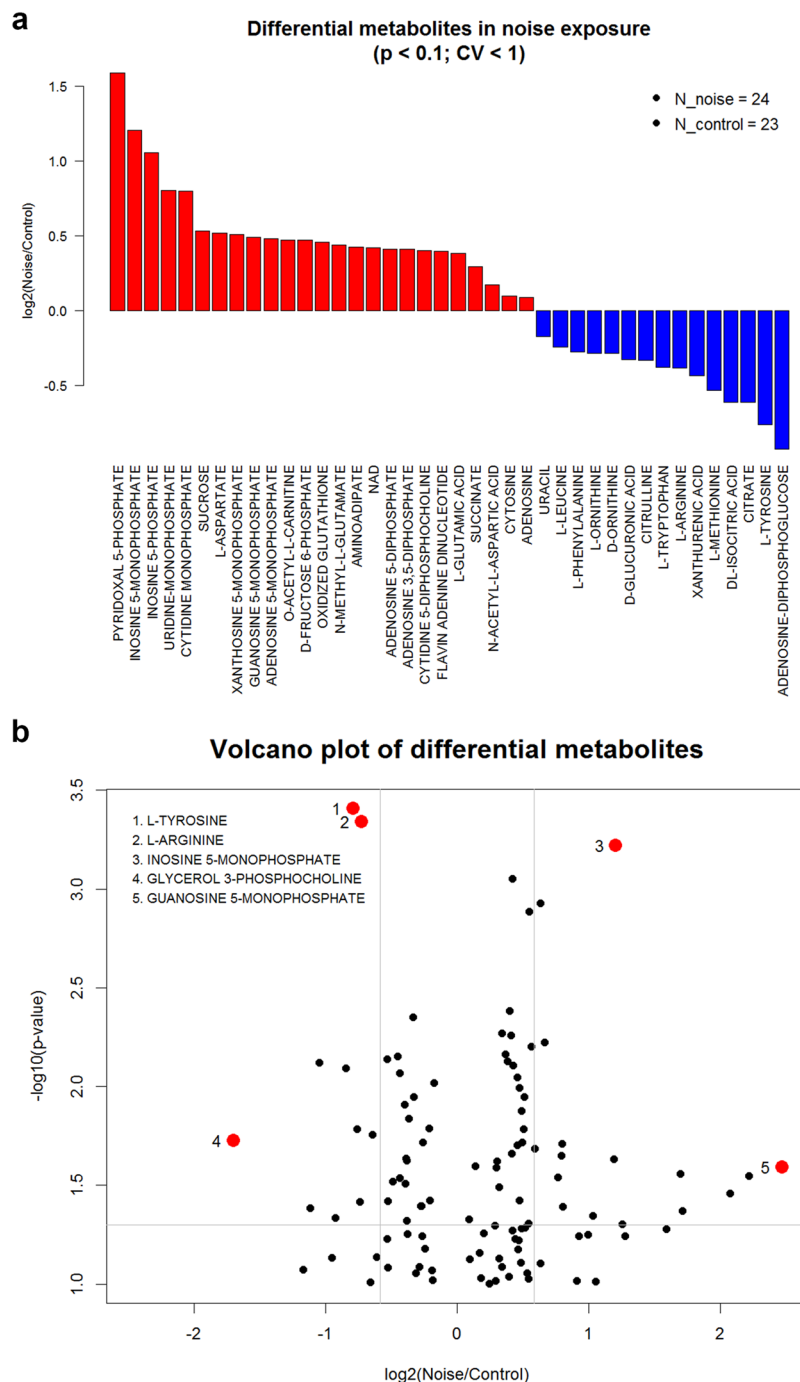


Figure 2. Metabolites altered by noise exposure. **(a)** Waterfall plot depicting the fold changes in the levels of metabolites affected by exposure to 100 dB SPL, 8–16 kHz for 2 hr. **(b)** Volcano plot of fold change vs. p-value. All differential metabolites are consistent in at least 2 experimental batches and the calculation of fold changes is based on median values of replicate measurements. See Supplementary Data for detailed values.

Metabolic changes depend on intensity and duration of noise exposure. The well-documented pathological effects of noise on inner ear structure and function are intensity- and duration-dependent². To test if the same is true for the effects of noise on the inner ear metabolome, we compared the effects of different types of exposures (Fig. 3). Representative results from four metabolites show a clear intensity-dependent effect (98, 100 or 110 dB SPL, 8–16 kHz, for 2 hr). As the noise intensity increases from 98 to 110 dB, so do the noise-induced changes in cytosine, N-methyl-L-glutamate, L-methionine and L-arginine. Similarly, representative results from three metabolites (Fig. 4) demonstrate that the effect of a 98 dB SPL, 8–16 kHz noise exposure depends on exposure duration (for 1 hr or 2 hr).

Pathway	P-value	FDR
Alanine, aspartate and glutamate metabolism	0.00045298	0.021229
Purine metabolism	0.00051779	0.021229
<i>Phenylalanine, tyrosine and tryptophan biosynthesis</i>	0.00046167	0.018928
<i>Phenylalanine metabolism</i>	0.0040809	0.11154

Table 1. Metabolic pathways altered by a 100 dB SPL, 8–16 kHz 2 hr noise exposure. The top 2 up-regulated (**bold**) and down-regulated (*italic*) metabolic pathways identified by the MetaboAnalyst webtool. P-value is calculated by a hypergeometric test. FDR = false discovery rate.

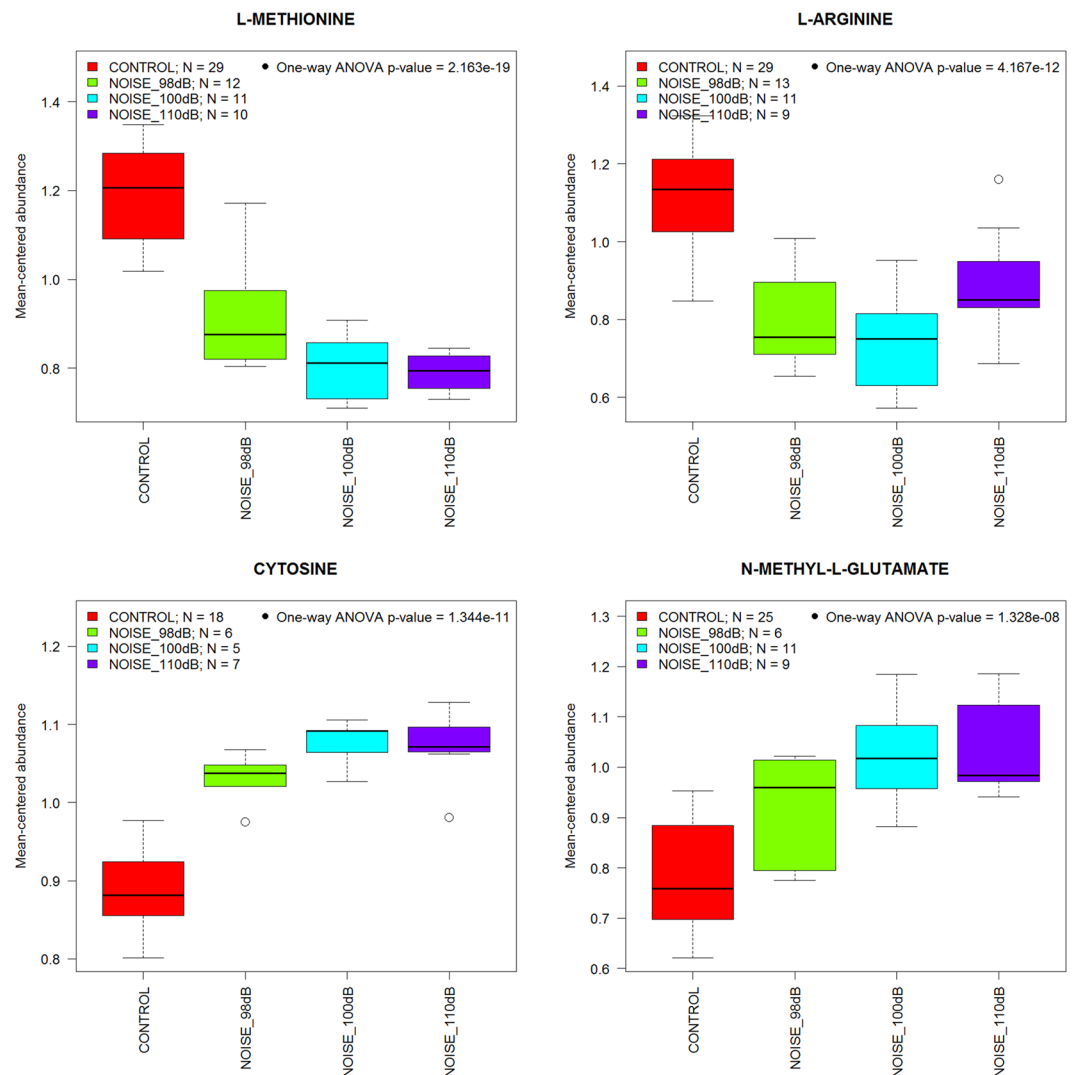


Figure 3. Intensity-dependent effects of noise on metabolite levels. The box-and-whisker plots illustrate that metabolic changes in the inner ear depend on the intensity of the sound presented (2 hours, 8–16 kHz band).

Meta-analysis for robustness and statistical power. In order to assess the robustness of the above results with more statistical power, we performed an additional analysis of the samples with 100 dB SPL noise for two hours and the corresponding control samples by pooling all control and exposed samples into two groups after metabolite-wise data standardization of each dataset, thereby increasing the sample size in each group, i.e., 15 samples per condition. We analyzed a subset of 186 metabolites that have less than 5 missing values in each of the exposed and control groups and CV < 1 in all replicate groups across all datasets. Our bioinformatic analysis yielded 39 differential metabolites, of which 17 were up-regulated and 22 were down-regulated (Fig. 5). Twenty-three of those 39 differential metabolites were also found in our individual batch-based analyses above, which include glutamate, methionine, arginine, tryptophan, xanthurenic acid, NAD⁺, and oxidized glutathione (GSSG).

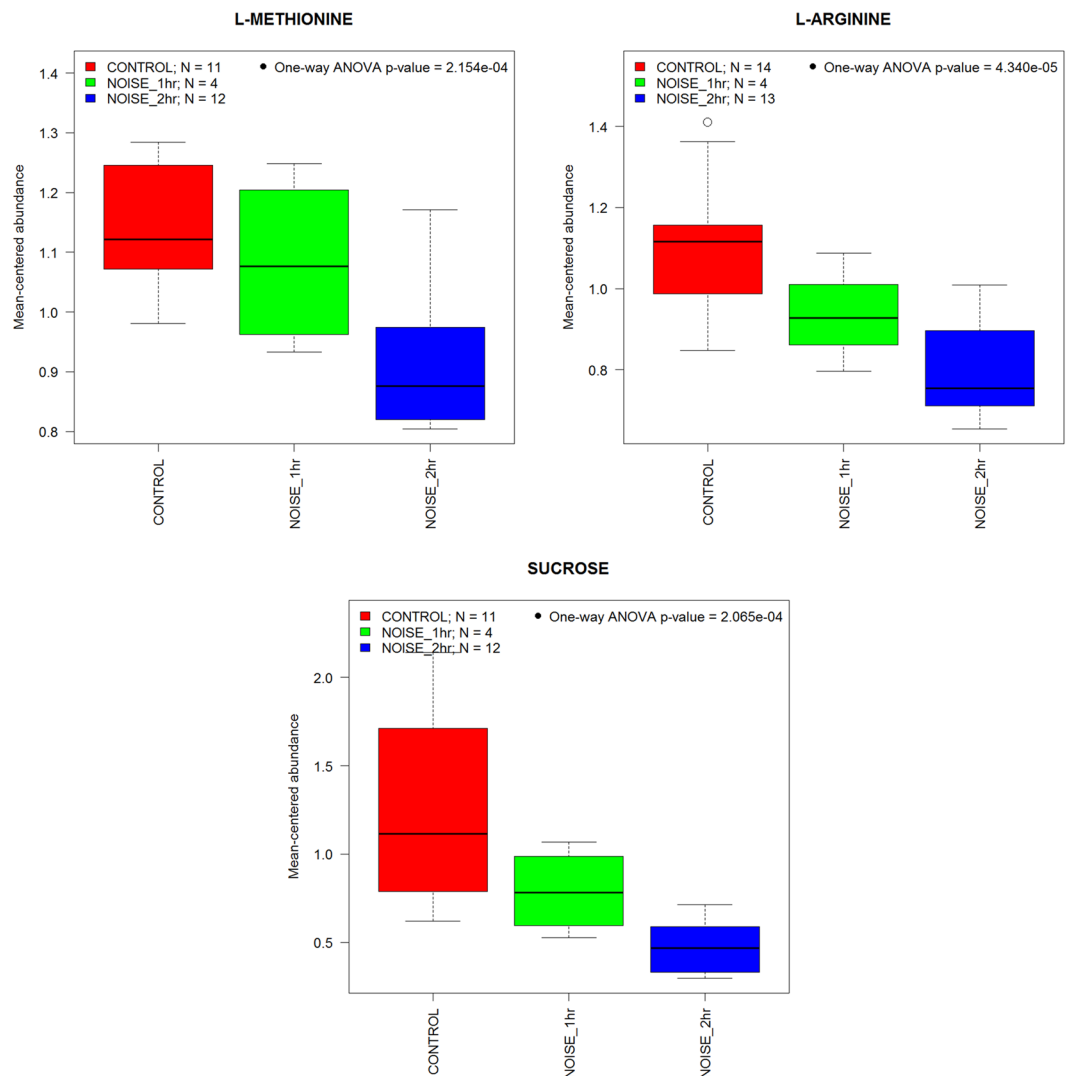


Figure 4. Duration-dependent effects of noise on metabolite levels. The box-and-whisker plots illustrate that metabolic changes in the inner ear depend on the duration of the exposure (98 dB SPL, 8–16 kHz band).

Discussion

Our results show that metabolomics profiling is a powerful approach for the characterization of inner ear metabolites in normal and pathological states. We found that noise exposure induces consistent and significant metabolic changes on an acute time scale. The results of our targeted metabolomics approach on the relative abundance of 220 metabolites in freshly harvested mouse inner ears both validate the procedure and provide novel insights into noise trauma. The fact that compounds related to cochlear neurotransmission and metabolic stress are clearly altered by noise underscores the validity of the methodology, as does the fact that the metabolic changes induced by noise depended on the intensity and duration of the exposure. Importantly, bioinformatics analysis identified several pathways previously unknown to be altered by noise, indicating that this technology can provide novel insights into the molecular events triggered by noise trauma.

Only two studies on inner ear metabolomics have been published previously. Fujita *et al.*¹⁵ measured the effects of a strong noise exposure (126 dB SPL) on the metabolome of guinea pig inner ear fluids while Mavel *et al.*¹⁶ analyzed the perilymph of humans who were undergoing cochlear implantation. We chose to analyze the whole mouse inner ear since at these early stages of technique development and exploration we believed it is imperative to consider the effects of noise broadly on metabolites in both intracellular and extracellular inner ear compartments. An added power of our approach is that future use of mouse models will provide tools to explore the relationship between a specific cell type (e.g., hair cells) or function (e.g., mechanotransduction) and the effects of pathological conditions on inner ear metabolism.

Our results on the effects of noise differ significantly from those of Fujita *et al.*¹⁵. Specifically, we measured the abundance of 220 metabolites, while their approach allowed for the detection of only 77. Consequently, we detected a larger number of noise-induced changes in inner ear metabolites, i.e. we identified 40 differential metabolites in whole inner ears while they only found 10 in inner ear fluids. Furthermore, more than half of our

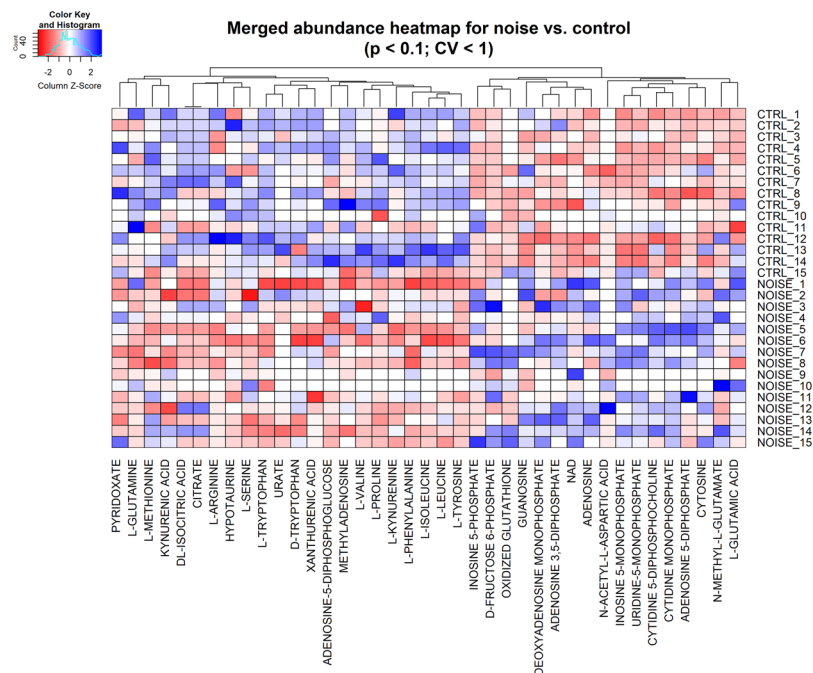


Figure 5. Meta-analysis of multiple datasets. Five metabolomics datasets from the three experiments with 100 dB SPL noise for 2 hours were analyzed by pooling all noise-exposed and control samples in two groups. Identification of differential metabolites and unsupervised hierarchical clustering were performed as in Fig. 1.

differential metabolites were undetectable in their experiment, and only 28% of metabolites altered by noise in our samples were detectable in theirs. The most parsimonious explanation is that the differences are due to the contents of inner ear tissues that are included in our samples although methodological disparities might have contributed. Importantly, in contrast to our analysis of the whole cochlea, Fujita *et al.*¹⁶ did not find effects of noise on neurotransmitters and compounds indicative of oxidative stress in guinea pig inner ear fluids, indicating that analysis of the cell compartments is critical.

Metabolomics has been also used to study the effects of noise exposure on the brain¹⁷. Interestingly, this study showed that a 1 h exposure to 16 kHz 110 dB SPL can cause long-lasting changes in the brain metabolome 6 months post-exposure. While the metabolic changes we observed in the inner ear are a direct effect of the sound, it is likely that the changes in the brain are a consequence of the noise-induced hearing loss.

The 220 metabolites we selected for analysis encompass the major pathways in central carbon metabolism and can thus be hypothesized as early indicators of pathological changes. Table 1 highlights the four pathways that showed the strongest statistical significance, as determined by pathway analysis for the top 40 altered metabolites identified using the MetaboAnalyst tool (<http://www.metaboanalyst.ca/>). Glutamate is the principal afferent neurotransmitter in the auditory system, mediating synaptic transmission between inner hair cells and afferent spiral ganglion neurons. Excess glutamate release and hyperactivation of glutamate receptors in the cochlea have been linked to excitotoxicity and damage to hair cells' afferent terminals^{18–20}. In particular, glutamate excitotoxicity has been suggested to contribute to the synaptic swelling seen after intense acoustic trauma (130 dB SPL)^{11,21,22}. However, previous studies failed to show a glutamate involvement during less intense exposures (100 dB or 105 dB SPL)^{21,23}. The up-regulation of glutamate in response to moderate noise (100 dB SPL) seen in our study extends the notion of glutamate excitotoxicity contributing to the pathogenesis of noise-induced HHL and synaptopathy. Xanthurenic acid (XA), an inhibitor of the glutamate vesicular transporter VGLUT²⁴, is down-regulated in our samples, suggesting that VGLUT activity might increase after noise. In addition to glutamate, aspartate is a major excitatory transmitter in the brain that is enriched in hair cells, afferent and efferent nerve fibers, and supporting cells in inner ear²⁵. Our observed increase after noise is consistent with Jaeger *et al.* and might be larger than or at least equal to the response of glutamate²³. Aspartate, therefore, could play a role similar to glutamate in inner ear metabolism and noise-induced hearing loss.

The indication that noise reduces phenylalanine, tyrosine and tryptophan biosynthesis is intriguing because a previous study showed that these aromatic amino acids suppress discharge by afferent fibers innervating hair cells in the lateral line of *Xenopus*²⁶. Thus, our data raise the question whether alterations in these amino acids are also at play in the mammalian cochlea and if they might contribute to vulnerability to noise.

It is likely that some of the noise-induced metabolic changes we observed reflect endogenous mechanisms of oto-protection. This might be the case for the noise-induced increases in ADP, AMP and adenosine levels (Fig. 2) as purinergic signaling has been suggested to protect from noise trauma and contribute to cochlear adaptation to elevated sound levels^{27,28}. Intense acoustic-overstimulation can increase inner ear purinergic signaling by enhancing agonist levels²⁹, increasing receptor levels³⁰, and upregulating the enzyme that catalyzes the breakdown of purinergic ligands, NTPDase^{31,32}. Adenosine signaling via the A1 receptor, which was shown to

Intensity (dB)	Duration (hour)	Number of mice
100	2	15
98	2	15
98	1	5
110	2	10

Table 2. Noise exposure intensity and duration used in this study.

be partially upregulated by noise in cochlear tissues³³, has also been linked to protection from noise-induced cochlear injury through the activation of antioxidant enzymes, inhibiting the release of neurotransmitters and promoting anti-apoptotic pathways^{34–37}.

The emergence of oxidative stress and its counterbalance by the action of antioxidant systems, well documented in noise trauma³⁸, also is reflected in our results. The increase in the oxidized form of the electron carriers NAD⁺ and FAD⁺ indicates a drain on reducing power which is underscored by an increase in oxidized glutathione, the major cellular antioxidant. Methionine, which is depleted following noise, can be recruited for the synthesis of glutathione or the provision of sulfhydryl groups via cysteine. The observation of decreased methionine also provides an explanation for the efficacy of supplementary methionine to attenuate noise- and drug-induced hearing loss in animal models^{38–40}.

In summary, we show that MS-based metabolomics is a powerful tool to study global metabolic effects induced by noise on the inner ear in mice. Noise exposures that result in hearing loss, hidden or overt, trigger acute metabolite abundance changes. It remains a challenge to answer the outstanding questions of which cell types give rise to the metabolic signatures and which of the changes are most significant and causal to the ensuing pathology. Towards this goal, we were able to identify differential inner ear metabolites and metabolic pathways that were significantly affected by noise depending on exposure intensity and duration. Most notably, our data have added to the understanding of the complex neurotransmission and modulation pathways altered by noise, and further supports the involvement of oxidative stress in noise trauma. This study therefore provides insights into the pathophysiology of NIHL from a metabolic perspective and offers novel opportunities to study pathogenesis, biomarker discovery, and to identify therapeutic strategies to block or treat disease.

Methods

Experimental groups and noise exposure. All animal procedures were approved by Institutional Animal Care and Use Committee of University of Michigan and all experiments were performed in accordance with relevant guidelines and regulations. For this study we used CBA/J mice with normal hearing housed in a facility with ambient sound levels of 40–50 dB within frequencies detectable by the mouse ear. Animals (8–12 weeks old) were randomly assigned to a control or noise exposed group (see Table 2). Control groups (n = 45) received no noise exposure. awake mice were placed within small cells in a subdivided cage, suspended in a reverberant noise exposure chamber. The stimulus was an exposure to an octave-band noise (8–16 kHz). Noise levels in different groups varied from 98 to 110 dB SPL and noise duration varied from 1 hour to 2 hours (Table 2). Noise calibration to target SPL was performed before each exposure session. Sound pressure levels varied by <1 dB across the cages.

Sample preparation. Temporal bones were harvested immediately after the exposure and the auditory bulla were isolated from the surrounding skull bone and placed in a Petri dish with phosphate buffered saline (PBS). We then quickly removed any attached musculature or soft tissue, the middle ear and the cerebellar paraflocculi to isolate the bony otic capsule containing the entire cochlea and vestibular organs (including sensory epithelia, sensory neurons, nerves, etc.) for processing. The round and oval windows were kept intact during the dissection to prevent dilution or contamination of the inner ear fluid with the bath solution.

Both inner ear tissues from a single mouse were placed together in an individual tube containing 1 ml of 80% methanol in water at –80 °C and stored at the same temperature. Samples of one batch (five exposed and five unexposed mice) were then simultaneously homogenized in their individual tubes using steel beads and a Qiagen Tissue Lyser (45 seconds at 28 Hz at room temperature). Samples were immediately brought back to –80 °C, after which insoluble material was centrifuged at 14,000 g at 4 °C. Supernatants were transferred to new tubes and subjected to Speedvac evaporation to obtain a dry pellet for liquid chromatography-coupled tandem mass spectrometry (LC-MS/MS) analysis.

Targeted metabolomics analysis. Metabolomics analysis was done using in-house protocols^{41,42}. Briefly, samples were analyzed using an Agilent 1290 UHPLC and 6490 Triple Quadrupole (QqQ) Mass Spectrometer (LC-MS/MS). We employed two LC methods: reversed-phase liquid chromatography (RPLC) and hydrophilic interaction liquid chromatography (HILIC). The RPLC separates hydrophobic or non-polar metabolites, while the HILIC separates polar or ionic metabolites. This approach generated two data sets per batch resulting in relative quantification ~220 metabolites across the major metabolic pathways in central carbon metabolism, including glycolysis, the TCA cycle, pentose phosphate pathway, amino acid and nucleotide metabolism, among others⁴².

Bioinformatic and statistical analysis. The pre-processed data of LC-MS/MS raw signals were post-processed to facilitate meta-analysis of differential metabolites from multiple datasets. We have developed a bioinformatic analysis pipeline in the R language based on our previous work⁴³. We first calculated coefficient of

variation (CV) across replicate samples for each metabolite given a cut-off value of signal peak areas in each dataset. We visually inspected distributions of CVs across multiple peak-area thresholds to identify the best threshold in each dataset as a noise cut-off value. Each sample was then normalized by the total intensity of all metabolites to correct for the moderate differences among tissue samples. Each metabolite abundance profile was scaled by the mean abundance across all samples for statistical analyses and visualizations. We performed a two-tailed t-test to identify metabolites with significant differences between exposed and control samples in each experiment. Differential metabolites were defined as those with p-values < 0.1 and CV < 1 among replicates. Metabolites were considered for further analysis if their profiles were consistent across the three experiments, and if present in at least half of all samples. Pathway analysis was performed using the MetaboAnalyst webtool⁴⁴.

References

1. Olusanya, B. O., Neumann, K. J. & Saunders, J. E. The global burden of disabling hearing impairment: a call to action. *Bull. World Health Organ.* **92**, 367–373 (2014).
2. Wang, Y., Hirose, K. & Liberman, M. C. Dynamics of noise-induced cellular injury and repair in the mouse cochlea. *J. Assoc. Res. Otolaryngol.* **3**, 248–268 (2002).
3. Kohrman, D. C., Wan, G., Cassinotti, L. & Corfas, G. Hidden Hearing Loss: A Disorder with Multiple Etiologies and Mechanisms. *Cold Spring Harb Perspect Med* a035493, <https://doi.org/10.1101/cshperspect.a035493> (2019).
4. Kujawa, S. G. & Liberman, M. C. Adding insult to injury: cochlear nerve degeneration after ‘temporary’ noise-induced hearing loss. *J. Neurosci.* **29**, 14077–14085 (2009).
5. Furman, A. C., Kujawa, S. G. & Liberman, M. C. Noise-induced cochlear neuropathy is selective for fibers with low spontaneous rates. *Journal of Neurophysiology* **110**, 577–586 (2013).
6. Kujawa, S. G. & Liberman, M. C. Synaptopathy in the noise-exposed and aging cochlea: Primary neural degeneration in acquired sensorineural hearing loss. *Hear. Res.* **330**, 191–199 (2015).
7. Liberman, M. C., Epstein, M. J., Cleveland, S. S., Wang, H. & Maison, S. F. Toward a Differential Diagnosis of Hidden Hearing Loss in Humans. *PLOS ONE* **11**, e0162726 (2016).
8. Wan, G., Gómez-Casati, M. E., Gigliello, A. R., Liberman, M. C. & Corfas, G. Neurotrophin-3 regulates ribbon synapse density in the cochlea and induces synapse regeneration after acoustic trauma. *eLife Sciences* **3**, e03564 (2014).
9. Ohlemiller, K. K., Wright, J. S. & Dugan, L. L. Early elevation of cochlear reactive oxygen species following noise exposure. *Audiol. Neurootol.* **4**, 229–236 (1999).
10. Ohinata, Y., Yamasoba, T., Schacht, J. & Miller, J. M. Glutathione limits noise-induced hearing loss. *Hear. Res.* **146**, 28–34 (2000).
11. Pujol, R. & Puel, J.-L. Excitotoxicity, Synaptic Repair, and Functional Recovery in the Mammalian Cochlea: A Review of Recent Findings. *Annals of the New York Academy of Sciences* **884**, 249–254 (1999).
12. Yamane, H. *et al.* Appearance of free radicals in the guinea pig inner ear after noise-induced acoustic trauma. *Eur Arch Otorhinolaryngol* **252**, 504–508 (1995).
13. Fujioka, M. *et al.* Proinflammatory cytokines expression in noise-induced damaged cochlea. *Journal of Neuroscience Research* **83**, 575–583 (2006).
14. Wakabayashi, K. *et al.* Blockade of interleukin-6 signaling suppressed cochlear inflammatory response and improved hearing impairment in noise-damaged mice cochlea. *Neuroscience Research* **66**, 345–352 (2010).
15. Fujita, T. *et al.* Metabolomic profiling in inner ear fluid by gas chromatography/mass spectrometry in guinea pig cochlea. *Neuroscience Letters* **606**, 188–193 (2015).
16. Mavel, S. *et al.* Validation of metabolomics analysis of human perilymph fluid using liquid chromatography-mass spectrometry. *Hearing Research* **367**, 129–136 (2018).
17. He, J. *et al.* Brain Metabolic Changes in Rats following Acoustic Trauma. *Front. Neurosci.* **11** (2017).
18. Hakuba, N., Koga, K., Gyo, K., Usami, S. & Tanaka, K. Exacerbation of Noise-Induced Hearing Loss in Mice Lacking the Glutamate Transporter GLAST. *J. Neurosci.* **20**, 8750–8753 (2000).
19. Hakuba, N. *et al.* Hearing loss and glutamate efflux in the perilymph following transient hindbrain ischemia in gerbils. *Journal of Comparative Neurology* **418**, 217–226 (2000).
20. Puel, J. L. Excitotoxicity and repair of cochlear synapses after noise-trauma induced hearing loss. *Neuroreport* **9**, 2109–2114 (1998).
21. Puel, J.-L., Pujol, R., Tribillac, F., Ladrech, S. & Eybalin, M. Excitatory amino acid antagonists protect cochlear auditory neurons from excitotoxicity. *Journal of Comparative Neurology* **341**, 241–256 (1994).
22. Pujol, R., Lenoir, M., Robertson, D., Eybalin, M. & Johnstone, B. M. Kainic acid selectively alters auditory dendrites connected with cochlear inner hair cells. *Hearing Research* **18**, 145–151 (1985).
23. Jäger, W. *et al.* Noise-induced aspartate and glutamate efflux in the guinea pig cochlea and hearing loss. *Exp Brain Res* **134**, 426–434 (2000).
24. Neale, S. A., Copeland, C. S., Uebele, V. N., Thomson, F. J. & Salt, T. E. Modulation of Hippocampal Synaptic Transmission by the Kynurenine Pathway Member Xanthurenic Acid and Other VGLUT Inhibitors. *Neuropsychopharmacology* **38**, 1060–1067 (2013).
25. Usami, S. & Ottersen, O. P. Aspartate is enriched in sensory cells and subpopulations of non-neuronal cells in the guinea pig inner ear: a quantitative immunoelectron microscopic analysis. *Brain Research* **742**, 43–49 (1996).
26. Mroz, E. A. & Sewell, W. F. Pharmacological alterations of the activity of afferent fibers innervating hair cells. *Hear. Res.* **38**, 141–162 (1989).
27. Housley, G. D. *et al.* ATP-gated ion channels mediate adaptation to elevated sound levels. *PNAS* **110**, 7494–7499 (2013).
28. Muñoz, D. J. B., Thorne, P. R. & Housley, G. D. P2X receptor-mediated changes in cochlear potentials arising from exogenous adenosine 5'-triphosphate in endolymph. *Hearing Research* **138**, 56–64 (1999).
29. Muñoz, D. J., Kendrick, I. S., Rassam, M. & Thorne, P. R. Vesicular storage of adenosine triphosphate in the guinea-pig cochlear lateral wall and concentrations of ATP in the endolymph during sound exposure and hypoxia. *Acta Otolaryngol.* **121**, 10–15 (2001).
30. Wang, J. *et al.* Noise induces up-regulation of P2X2 receptor subunit of ATP-gated ion channels in the rat cochlea. *Neuroreport* **14**, 817–823 (2003).
31. Vlajkovic, S. M. *et al.* Noise-induced up-regulation of NTPDase3 expression in the rat cochlea: Implications for auditory transmission and cochlear protection. *Brain Research* **1104**, 55–63 (2006).
32. Vlajkovic, S. M. *et al.* Noise exposure induces up-regulation of ecto-nucleoside triphosphate diphosphohydrolases 1 and 2 in rat cochlea. *Neuroscience* **126**, 763–773 (2004).
33. Ramkumar, V., Whitworth, C. A., Pingle, S. C., Hughes, L. F. & Rybak, L. P. Noise induces A1 adenosine receptor expression in the chinchilla cochlea. *Hearing Research* **188**, 47–56 (2004).
34. Fredholm, B. B. Adenosine, an endogenous distress signal, modulates tissue damage and repair. *Cell Death and Differentiation* **14**, 1315–1323 (2007).
35. Linden, J. Adenosine in Tissue Protection and Tissue Regeneration. *Mol Pharmacol* **67**, 1385–1387 (2005).
36. Maggirwar, S. B., Dhanraj, D. N., Somani, S. M. & Ramkumar, V. Adenosine Acts as an Endogenous Activator of the Cellular Antioxidant Defense System. *Biochemical and Biophysical Research Communications* **201**, 508–515 (1994).

37. Ramkumar, V., Nie, Z., Rybak, L. P. & Maggirwar, S. B. Adenosine, antioxidant enzymes and cytoprotection. *Trends in Pharmacological Sciences* **16**, 283–285 (1995).
38. Sha, S.-H. & Schacht, J. Emerging therapeutic interventions against noise-induced hearing loss. *Expert Opin Investig Drugs* **26**, 85–96 (2017).
39. Campbell, K. C. M. *et al.* Prevention of noise- and drug-induced hearing loss with D-methionine. *Hearing Research* **226**, 92–103 (2007).
40. Sha, S.-H. & Schacht, J. Antioxidants attenuate gentamicin-induced free radical formation *in vitro* and ototoxicity *in vivo*: D-methionine is a potential protectant. *Hearing Research* **142**, 34–40 (2000).
41. Yuan, M. *et al.* *Ex vivo* and *in vivo* stable isotope labelling of central carbon metabolism and related pathways with analysis by LC–MS/MS. *Nature Protocols* **14**, 313 (2019).
42. Lee, H.-J., Kremer, D. M., Sajjakulnukit, P., Zhang, L. & Lyssiotis, C. A. Meta-analysis of targeted metabolomics data from heterogeneous biological samples provides insights into metabolite dynamics. *bioRxiv* 509372, <https://doi.org/10.1101/509372> (2019).
43. Halbros, C. J. *et al.* Macrophage-Released Pyrimidines Inhibit Gemcitabine Therapy in Pancreatic Cancer. *Cell Metabolism*, <https://doi.org/10.1016/j.cmet.2019.02.001> (2019).
44. Chong, J. *et al.* MetaboAnalyst 4.0: towards more transparent and integrative metabolomics analysis. *Nucleic Acids Res.* **46**, W486–W494 (2018).

Acknowledgements

This study was supported by NIH/NIDCD (No. R01DC004820 to G.C.); a Dale F. Frey Award for Breakthrough Scientists from the Damon Runyon Cancer Research Foundation (DFS-09-14 to C.A.L.); a Junior Scholar Award from The V Foundation for Cancer Research (V2016-009 to C.A.L.); a Kimmel Scholar Award from the Sidney Kimmel Foundation for Cancer Research (SKF-16-005 to C.A.L.); and a China Scholarship Council (No. 201508110245 to L.J.). Metabolomics studies performed at the University of Michigan were supported by NIH grant DK097153.

Author Contributions

G.C. and C.L. conceived the study, L.J., G.W., G.P.W., L.Z. and P.S. performed experiments, H.-J.L. performed the data analysis. All authors contributed to data interpretation and manuscript writing.

Additional Information

Supplementary information accompanies this paper at <https://doi.org/10.1038/s41598-019-45385-8>.

Competing Interests: G.C. is a scientific founder of Decibel Therapeutics, has an equity interest in and has received compensation for consulting, but the company was not involved in this study.

Publisher's note: Springer Nature remains neutral with regard to jurisdictional claims in published maps and institutional affiliations.



Open Access This article is licensed under a Creative Commons Attribution 4.0 International License, which permits use, sharing, adaptation, distribution and reproduction in any medium or format, as long as you give appropriate credit to the original author(s) and the source, provide a link to the Creative Commons license, and indicate if changes were made. The images or other third party material in this article are included in the article's Creative Commons license, unless indicated otherwise in a credit line to the material. If material is not included in the article's Creative Commons license and your intended use is not permitted by statutory regulation or exceeds the permitted use, you will need to obtain permission directly from the copyright holder. To view a copy of this license, visit <http://creativecommons.org/licenses/by/4.0/>.

© The Author(s) 2019